A Synthetic Strategy for the Construction of Zeolite-Entrapped Organized Molecular Assemblies. Preparation and Photophysical Characterization of Interacting Adjacent Cage Dyads Comprised of Two Polypyridine Complexes of Ru(II)

Milan Sykora, Krzysztof Maruszewski, Shelly M. Treffert-Ziemelis, and James R. Kincaid*

Contribution from the Chemistry Department, Marquette University, Milwaukee, Wisconsin 53201-1881

Received October 15, 1996. Revised Manuscript Received February 6, 1998

Abstract: A novel synthetic strategy for the preparation of organized molecular assemblies entrapped within the supercage network of Y-zeolite is described. A molecular assembly composed of two Ru(II)−polypyridine complexes, $Ru(bpy)_2bpz^{2+}$ and $Ru(mmb)_3^{2+}$ (where bpy = 2,2′-bipyridine, bpz = 2,2′-bipyrazine, and mmb = 5-methyl-2,2′-bipyridine), entrapped in adjacent supercages, has been prepared and characterized by diffuse reflectance, resonance Raman and electronic emission spectroscopy, and excited-state lifetime measurements. A dramatic (∼2.5−4-fold) decrease in the emission intensity of the adjacent cage assembly, compared to a sample in which the two complexes are distributed randomly (RM) or in separate particles (MM), indicates strong interaction between the adjacent complexes. The results of the excited-state lifetime measurements are consistent with this observation. Thus, in the emission decay profile of the assembly, a new short-lived component (∼30 ns), attributable to the emission from the interacting dyad molecules, has been observed. While this short component dominates the emission decay for the adjacent cage assembly, it is not observed in the mechanical mixture (MM) and is too small to be accurately determined in the randomized sample (RM).

Introduction

There is a long, well-documented history of the use of zeolites as supports for entrapped or adsorbed transition metal catalysts or photocatalysts.[1−3] These zeolitic supports are aluminosilicates whose three-dimensional structure is made up of corner sharing SiO_4 and AlO_4 tetrahedra, with exchangeable cations (M^{n+}) occupying extraframework positions to neutralize charge.[4] One of the most commonly employed materials, Y-zeolite, possesses a three-dimensional framework that is comprised of "supercages" of 13 Å internal diameter, each of which is connected to four other, tetrahedrally arranged, supercages by 12-membered-ring openings having 7−8 Å "windows".

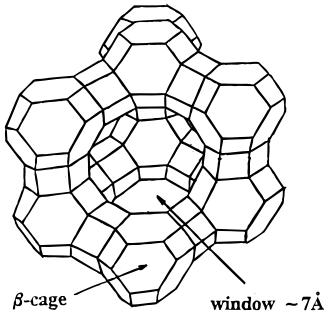

Supercage size ~13 Å

To clarify later discussion, it is noted that the four supercages surrounding a given central cage do not share a common window with any of the other four; i.e., these four supercages are not adjacent to one another. The relatively large size of the supercages of such materials makes them especially attractive as hosts for transition metal catalysts and much attention has been focused on the preparation and characterization of such zeolite-entrapped transition metal complexes. Lunsford and coworkers[5] were the first to show that the familiar photosensitizer,[6] $Ru(bpy)_3^{2+}$, could be synthesized (and thereby entrapped) within the supercages of Y-zeolite via a "ship-in-the-bottle" approach. In recent years, we have expanded this approach by devising

(1) (a) Lunsford, J. *ACS Symp. Ser.* **1977**, *40*, 473. (b) Kalyanasundaram, K. *Photochemistry in Microheterogeneous Systems*; Academic Press: Orlando, FL, 1987. (c) *Photochemistry in Organized and Constrained Media;* Ramamurthy, V., Ed.; VCH: New York, 1991. (d) De Vos, D. E.; Knops-Gerrits, P. P.; Parton, R. F.; Weckhuysen, B. M.; Jacobs, P. A.; Schoonheydt, R. A. *J. Inclusion Phenom. Mol. Recogn. Chem.* **1995**, *21*, 185. (e) Bedoui, F. *Coord. Chem. Rev.* **1995**, *144*, 39.

(2) (a) Faulkner, L. R.; Suib, S. L.; Renschler, L. L.; Green, J. M.; Bross, P. R. In *Chemistry in energy production*; Wymer, R. G., Keller, O. L., Eds.; ACS Symp. Ser. 99; American Chemical Society: Washington, DC, 1982. (b) Li, Z.; Wang, C. H.; Persaud, L.; Mallouk, T. E. *J. Phys. Chem.* **1988**, *92*, 2592. (c) Kruger, J. S.; Mayer, J. A.; Mallouk, T. E. *J. Am. Chem. Soc.* **1988**, *110*, 8232. (d) Kim, Y. I.; Mallouk, T. E. *J. Phys. Chem.* **1992**, *96*, 2879. (e) Turbeville W.; Robins, D. S.; Dutta, P. K. *J. Phys. Chem.* **1992**, *96*, 5024.

(3) (a) Dutta, P. K.; Incavo, *J. A. J. Phys. Chem.* **1987**, *91*, 4443. (b) Dutta, P. K.; Turbeville, W. *J. Phys. Chem.* **1992**, *96*, 9410. (c) Borja, M.; Dutta, P. K. *Nature* **1993**, *362*, 43. (d) Dutta, P. K.; Borja, M.; Ledney, M. *Sol. Energy Mater. Sol. Cells* **1995**, *38*, 239.

(4) (a) Breck, D. W. *Zeolite Molecular Sieves*: *Structure Chemistry and Use*; Wiley: New York, 1974. (b) *Zeolites and Related Materials: State of the Art*; Weitcamp, J., Karge, H. G., Pfeifer, H., Holderich, W., Eds.; Elsevier: Amsterdam, 1994.

(5) (a) DeWilde, W.; Peeters, G.; Lunsford, J. H. *J. Phys. Chem.* **1980**, *84*, 2306. (b) Quayle, W. H.; Lunsford, J. H. *Inorg. Chem.* **1982**, *21*, 97.

(6) (a) *Photochemical Conversion and Storage of Solar Energy*; Norris, J. R., Jr., Meisel, D., Eds.; Elsevier: Amsterdam, 1988. (b) Kalyanasundaram, K. *Photochemistry of Polypyridine and Porphyrin complexes*; Academic Press: San Diego, 1992. (c) Juris, A.; Balzani, V.; Barigelletti, F.; Campagna, S.; Belser, P.; Von Zelewsky, A. *Coord. Chem. Rev.* **1988**, *84*, 85. (c) Meyer, T. J. *Acc. Chem. Res.* **1989**, *22*, 163. (d) Grätzel, M. *Acc. Chem. Res.* **1981**, *14*, 376. (e) Amouyal, E. *Sol. Energy Mater. Sol. Cells* **1995**, *38*, 249.

S0002-7863(96)03584-6 CCC: $15.00
Published on Web 03/19/1998

methods to prepare structurally diverse zeolite-entrapped complexes of divalent ruthenium and have carefully documented their spectroscopic and photophysical properties.[7] Dutta and co-workers[3,8] have further studied the photophysical properties of zeolite-entrapped $Ru(bpy)_3^{2+}$ (Z-$Ru(bpy)_3$) and have shown the value of such systems for obtaining long-lived net charge separation upon photoinduced electron transfer from the excited sensitizer to intrazeolitic[3a,b] and solution phase[3c] acceptors. Herron and co-workers,[9] as well as others,[10] have prepared zeolite-entrapped complexes of phthalocyanines and documented their effectiveness for catalysis of small molecule oxidative chemistry. More recently, various complexes of manganese and iron have been prepared within the supercages of Y-zeolite.[11]

In all of these previous studies, the complexes were introduced to, or synthesized within, the zeolite cages in a purely statistical (randomized) arrangement. Herein we report a novel synthetic strategy for the construction of more elaborately organized, multicomponent, intrazeolitic catalytic systems, wherein two (or potentially more) individual complexes can be arranged, both spatially and in terms of reactivity, to possibly enhance catalytic efficiency. Specifically, it is shown that intrazeolitic transition metal complexes which possess ligands bearing peripheral donor atoms (e.g., Z-$Ru(bpy)_2$(bpz), where bpz is 2,2′-bipyrazine) are susceptible to coordination by an ammine complex of divalent ruthenium, $[Ru(NH_3)_5(H_2O)]^{2+}$; chemistry which parallels that previously described by Lever and co-workers in solution phase work.[12] These metalated, zeolite-entrapped, tris-ligated complexes (e.g., Z-$Ru(bpy)_2$bpz-$Ru(NH_3)_5$) can be further treated with excess chelating agent, e.g., 2,2′-bipyridine. Upon heating, the peripheral $Ru-N_{bpz}$ bond is ruptured and a second transition metal complex (e.g., $Ru(bpy)_3^{2+}$) is formed and trapped in the supercage immediately adjacent to that containing the original bis-heteroleptic, tris-ligated complex (i.e., $Ru(bpy)_2(bpz)^{2+}$, in the above example).

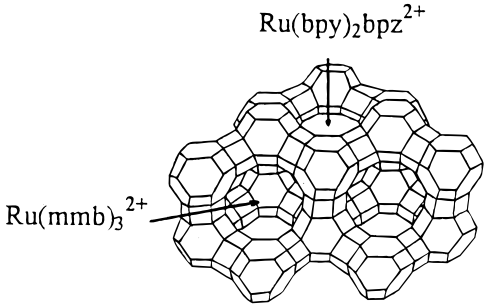

Spectroscopic analysis confirms the integrity of such materials and detailed photophysical studies document a strong interaction between such adjacent cage dyads.

Experimental Section

A. Materials. The Y-zeolite used in this study was generously provided by Union Carbide Corp. Prior to use the crude zeolite was purified from organic impurities by oxidation under a flow of oxygen at 500 °C for 6 h.[8] The so-called "calcinated" zeolite was then extensively washed with 10% (w/v) NaCl and deionized water. The complexes $RuCl_3 \cdot 3H_2O$ and $[Ru(NH_3)_6]Cl_3$ were purchased from Aldrich Chemical Co. and used without further purification. All solvents used were reagent grade or better.

B. Preparation of Compounds. 1. Ligands. The ligand 2,2′-bipyridine (bpy) was purchased from Aldrich Chemical Co. and was sublimed prior to use. The ligands 2,2′-bipyrazine[13] and 5-monomethyl-2,2′-bipyridine[14] were prepared following literature procedures.

2. Complexes in Solution. The $[Ru(bpy)_2bpz](PF_6)_2$ was prepared from $RuCl_3 \cdot 3H_2O$ by a standard procedure.[15] $[Ru(NH_3)_5(H_2O)](PF_6)_2$ was prepared from $[Ru(NH_3)_5Cl]Cl_2$ by a procedure originally described by Taube and co-workers.[16] The precursor complex $[Ru(NH_3)_5Cl]Cl_2$ was prepared from $[Ru(NH_3)_6]Cl_3$ following the procedure described by Vogt et al.[17] $[Ru(bpy)_2bpz\text{-}Ru(NH_3)_5](PF_6)_4$ was prepared by reacting $[Ru(bpy)_2bpz](PF_6)_2$ with an equimolar amount of $[Ru(NH_3)_5(H_2O)](PF_6)_2$, following the procedure reported for the preparation of $[Ru(bpz)_3\text{-}Ru(NH_3)_5](PF_6)_2$ by Lever et al.[12] Elemental analysis calcd for $[Ru(bpy)_2bpz\text{-}Ru(NH_3)_5](PF_6)_4 \cdot 3(CH_3)_2CO$: C, 29.39; N, 12.04; H, 3.13. Found: C, 29.90; N, 12.37; H, 3.01.

3. Zeolite-Entrapped Complexes. The zeolite-entrapped complexes Z-$Ru(bpy)_2$bpz and Z-$Ru(mmb)_3$ were prepared by using modified methods previously developed in our laboratory,[7] which are based on the pioneering work of Lunsford and co-workers.[5] The randomized mixture was prepared by following the same procedure in a stepwise manner, i.e., the Z-$Ru(mmb)_3$ was first prepared and in the second step the Z-$Ru(bpy)_2$bpz was synthesized within the zeolite particles previously loaded with $Ru(mmb)_3^{2+}$.

4. Adjacent Cage Assembly. *Z-Ru(bpy)$_2$bpz-Ru(NH$_3$)$_5$*, used as the precursor for the adjacent cage assembly, was prepared by a modification of the procedure previously reported[12] for the preparation of $[Ru(bpz)_3\text{-}Ru(NH_3)_5](PF_6)_2$ in solution. Since this type of synthesis is now adapted, for the first time, for the zeolite matrix, we describe the synthetic procedure in detail.

Typically 0.5 g of sand-yellow Z-$Ru(bpy)_2$bpz was evacuated at ~160 °C overnight and then allowed to cool to room temperature under vacuum. Approximately 30 mL of degassed acetone (5 to 6 freeze−pump−thaw cycles) was then vacuum distilled into the evacuated flask containing the zeolite. The flask was then filled with argon. A 100-fold molar excess of $[Ru(NH_3)_5H_2O](PF_6)_2$ (with respect to the entrapped $Ru(bpy)_2bpz^{2+}$) was then added to the Z-$Ru(bpy)_2$bpz−acetone suspension under an argon atmosphere. The reaction mixture, suspended in acetone, was then stirred under Ar for 1 h in order to ion exchange the $[Ru(NH_3)_5H_2O]^{2+}$ into the zeolite. During this time the color of the stirred suspension changed from yellow-orange to brown. Then the mixture was refluxed at 60 °C for an additional 1 h, under an inert atmosphere, whereupon the suspension turned dark brown. Finally, the acetone was evaporated to dryness, under a vigorous stream of argon. The solid (light blue-green) residue was then washed under an argon atmosphere with 200 mL of degassed acetone, 3 L of 25% (w/v) NaCl (in order to remove excess unreacted $[Ru(NH_3)_5H_2O]^{2+}$), and 500 mL of deionized water. The light blue product, Z-$Ru(bpy)_2$bpz-$Ru(NH_3)_5$, was finally dried on a vacuum line at room temperature.

We would like to note that the requirement to maintain an inert atmosphere throughout the synthetic and purification steps is critical,

(7) (a) Maruszewski, K.; Strommen, D. P.; Handrich, K.; Kincaid, J. R. *Inorg. Chem.* **1991**, *30*, 4579. (b) Maruszewski, K.; Strommen, D. P.; Kincaid, J. R. *J. Am. Chem. Soc.* **1993**, *115*, 8345. (c) Maruszewski, K.; Kincaid, J. R. *Inorg. Chem.* **1995**, *34*, 2002.

(8) Incavo, J. A.; Dutta, P. K. *J. Phys. Chem.* **1990**, *94*, 3075.

(9) (a) Herron, N. *Inorg. Chem.* **1986**, *25*, 4714. (b) Herron, N.; Stucky, G. D.; Tolman, C. A. *J. Chem. Soc., Chem. Commun.* **1986**, 1521. (c) Herron, N. *J. Coord. Chem.* **1988**, *19*, 25.

(10) (a) See refs 61−89 in ref 1e. (b) Paez-Mozo, E.; Gabriunas, N.; Lucaccioni, F.; Acosta, D. D.; Patrono P.; La Ginestra, A.; Ruiz, P.; Delmon, B. *J. Phys. Chem.* **1993**, *97*, 12819. (c) Wöhrle, D.; Sobbi, A. K.; Franke, O.; Schulz-Eklofff, G. *Zeolites* **1995**, *15*, 540.

(11) (a) Knops-Gerrits, P. P.; De Schryver, F. C.; Van Der Auweraer, M.; Van Mingroot, H.; Li, X.; Jacobs, P. A. *Chem. Eur. J.* **1996**, *2*, 592. (b) Umemura, Y.; Minai, Y.; Tominaga, T. *J. Chem. Soc., Chem. Commun.* **1993**, 1822. (c) Parton, R. F.; Uytterhoeven, L.; Jacobs, P. A. *Stud. Surf. Sci. Catal.* **1991**, *59*, 395. (d) Parton, R. F.; Huybrechts, D. R. C.; Buskens, P.; Jacobs, P. A. *Stud. Surf. Sci. Catal.* **1991**, *65*, 110.

(12) Toma, H. E.; Auburn, P. R.; Dodsworth, E. S.; Golovin, M. N.; Lever, A. B. P. *Inorg. Chem.* **1987**, *26*, 4257.

(13) Crutchley, R. J.; Lever, A. B. P. *Inorg. Chem.* **1982**, *21*, 2276.

(14) (a) Huang, T. L. J.; Brewer, D. G. *Can J. Chem.* **1981**, *59*, 1968. (b) Treffert-Ziemelis, S. M.; Kincaid, J. R. *J. Raman Spectrosc.* **1994**, *25*, 893.

(15) McClanahan, S. F.; Dallinger, R. F.; Holler, F. J.; Kincaid, J. R. *J. Am. Chem. Soc.* **1985**, *107*, 4853.

(16) Kuehn, C. G.; Taube, H. J. *J. Am. Chem. Soc.* **1976**, *98*, 689.

(17) Vogt, L. H.; Katz, J. L.; Wiberley, S. E. *Inorg. Chem.* **1965**, *4*, 1157.

inasmuch as the $[Ru(NH_3)_5H_2O](PF_6)_2$, especially when dissolved in acetone, is extremely sensitive to traces of O_2. Upon oxidation the complex forms a very intense purple trimer of "ruthenium-red" $[(NH_3)_5Ru^{III}-O-Ru^{IV}(NH_3)_4-O-Ru^{III}(NH_3)_5]^{6+}$. An indication of Ru-red contamination of the product is the presence of a purple color in the acetone and NaCl washings in the final step of the synthetic procedure. In the absence of the impurity, the washings have a yellow color (characteristic of $[Ru(NH_3)_5H_2O](PF_6)_2$).

The adjacent cage assembly *Z-{Ru(bpy)$_2$bpz}{Ru(mmb)$_3$}* was prepared from the precursor material, Z-Ru(bpy)$_2$bpz-Ru(NH$_3$)$_5$, by the following procedure.

Typically the 0.5 g of Z-Ru(bpy)$_2$bpz-Ru(NH$_3$)$_5$ and 20 drops (from a Pasteur pipet) of neat 5-mmb (∼0.5 g) was suspended in 2 mL of 95% EtOH in a 2 × 10 cm Pyrex reaction tube and stirred at ∼4 °C overnight. The ethanol was then evaporated under a stream of nitrogen. The solid residue was then evacuated (3 min) and flushed with nitrogen 3 times and finally evacuated at $\sim 10^{-3}$ Torr for 10 min. The tube was then inserted into a (room temperature) oil bath that was slowly (over a period of ∼12 h) warmed to 200 °C. During this time the color of zeolite slowly changed from blue to yellow-orange, indicating decomposition of the binuclear complex and formation of entrapped Ru(mmb)$_3^{2+}$. The heating at 200 °C was then continued for an additional 24 h. The sample was then allowed to cool to room temperature. The product was extensively washed with 10% NaCl, deionized water, and ethanol and then extensively Soxhlet extracted with 95% EtOH (10−14 days). The washings of EtOH were periodically checked by electronic absorption spectrophotometry for the presence of 5-mmb (λ_{max} at ∼286 nm) until no trace of ligand could be detected. Finally, the product was washed with 10% NaCl and deionized water and air-dried.

5. Preparation of "Z-Ru-red". A sample of Z-Ru-red used for diffuse reflectance measurements was prepared by adding a small amount of the yellow $[Ru(NH_3)_5(H_2O)](PF_6)_2$ to a suspension of calcinated Na−Y-zeolite in acetone. After continuous stirring for a period of 3 h in air the intense purple suspension was filtered and allowed to air-dry. We would like to note that this procedure (unlike procedures described in previous paragraphs) can yield a considerable amount of the zeolite surface adsorbed complex, inasmuch as the formation of the purple trimer is rapid and can occur on the time scale comparable to the ion-exchange of the monomer into the zeolite.

C. Physical Measurements. 1. Electronic Absorption Spectra. Electronic absorption spectra in the UV−visible region were recorded on a Hewlett-Packard 8452A diode array spectrometer. Spectra were recorded in the absorbance mode.

To determine the total amounts of the entrapped complex in the mechanical mixture (MM), randomized mixture (RM), and adjacent cage assembly (AC), the absorption spectra of the complexes liberated from the zeolite by the previously described hydrofluoric acid method[7a] were acquired. Thus, identical amounts (10 mg) of each of the zeolitic sample were dissolved in 1 mL of diluted HF and subsequently neutralized with 1 mL of 2 M NaOH. The solutions were then centrifuged to separate precipitated white silicate. The absorption spectrum of each extract was then recorded and the absorbance of the band near 450 nm was compared.

To determine the extent of the contamination of the zeolitic samples by trace organic impurities possibly present in the zeolite even after extensive Soxhlet purification the acquisition of the absorption spectra in the UV region is desirable. Since with the instrumentation available to us (vide supra) we were unable to acquire diffuse reflectance spectra in the UV region directly on the zeolitic samples, the following procedure was employed.

A small amount of Z-{Ru(bpy)$_2$bpz}·{Ru(mmb)$_3$} (adjacent cage assembly) was dissolved in diluted HF.[7a] The extract was then neutralized with 2 M NaOH and diluted to a total volume of 5 mL with deionized water. This solution was then extracted with 5 mL of CH_2Cl_2. Neither of the extracts has been further diluted prior the absorption measurements. The UV−vis spectra of both the aqueous and the organic phase were measured in the region 220−820 nm.

2. Diffuse Reflectance Spectra. Diffuse reflectance spectra were recorded on a Perkin-Elmer 320 spectrophotometer equipped with a Hitachi integrating sphere attachment. The zeolite samples were measured as KBr pellets, where the pellet with an identical content of plain Na−Y-zeolite was used as blank. Finely ground $BaSO_4$ was used as a reference. The spectra, recorded in the transmittance mode, were numerically Kubelka−Munk corrected by using facilities of the Spectracalc Software.

3. Electronic Emission Spectra. Zeolite samples (∼50 mg) were transferred into 5 mm i.d. NMR tubes, degassed at $\sim 10^{-4}$ Torr overnight, then exposed to vapors of degassed (3 × freeze−pump−thaw) deionized water. Two more F−P-T cycles were then performed on the suspension and the sample was finally sealed inside the NMR tube on the vacuum line. Electronic emission spectra were obtained by using a conventional Raman spectrometer (Spex Model 1403 double monochromator equipped with a Spex Model DM1B controller and Hammamatsu R928 photomultiplier tube) with a Spectra-Physics Model 2025-05 argon ion laser as the excitation source. The spinning 5 mm i.d. NMR tube was illuminated by a laser beam focused through a glass lens (typical power at the sample was 5−10 mW) and the emission from the sample was collected with a conventional two-lens collecting system. After recording a single scan for each of the measured samples, the emission intensity at the respective emission maxima has been monitored repeatedly. Typically, the results of 10 measurements for each sample have been averaged and the resulting value was considered to be the observed emission intensity. To avoid fluctuations in the excitation power, during these measurements, the laser was used in the constant power mode.

4. Resonance Raman Spectra. Resonance Raman spectra were obtained by using the same instrumental setup as described for the electronic emission spectra. The 457.9 nm line from the argon ion laser was used for excitation. Spectra of zeolite-entrapped compounds were obtained from the solid samples in spinning NMR tubes.

5. Excited-State Lifetimes. The samples for lifetime measurement were freshly degassed following the procedure used for emission measurements. The third harmonic (354.7 nm; fwhm = 16 ns) of a Quanta-Ray (Spectra-Physics) Model GCR-11 Nd:YAG laser (operated at 20 Hz) with the beam defocused (∼2 mm diameter) was used as the excitation source for the lifetime measurements (power at the sample was in all cases below 0.05 mJ/pulse). The light emitted from the sample in the spinning NMR tube was transferred through glass collecting and transferring lenses and a 580 nm cutoff filter to a SPEX 340S spectrometer equipped with an RCAC31034A-02 photomultiplier tube with −1800 V applied voltage. The PMT output signal was directed to a LeCroy 9450A Dual 300 MHz oscilloscope. The emission was in all cases monitored at 620 nm. The temperature change in the laboratory did not exceed ±0.3 K during the measurement. In all reported cases, 3000 scans of the emission decay curve were averaged and transferred to the computer. The curves were then fitted (within a minimum of 4 lifetimes) by a mono- or multiexponential model (vide supra) with commercial software (PSI−Plot) based on the Marquardt−Levenberg algorithm. The quality of the fit for a particular model was monitored by comparing plots of the residuals between the experimental and the fitted curve. The number of exponential terms was, if necessary, increased from 1 up to 3 until the maximum residual values were below 1% and symmetrically distributed around the zero value.

Results and Discussion

A. Characterization of Z-Ru(bpy)$_2$bpz-Ru(NH$_3$)$_5$. The diffuse reflectance spectra of the Z-Ru(bpy)$_2$bpz and the product of its reaction with $[Ru(NH_3)_5(H_2O)](PF_6)_2$ are shown in Figure 1. The spectra of the latter are similar to those reported for Ru(bpz)$_3$-Ru(NH$_3$)$_5$ by Lever and co-workers,[12] suggesting coordination of one peripheral nitrogen of bpz to the Ru(NH$_3$)$_5$ fragment. The characteristic feature in the absorption spectrum, indicating this attachment, is the appearance of a new broad absorption band near 650 nm, which is ascribable to the metal-to-ligand charge transfer transition associated with the externally attached Ru(NH$_3$)$_5$ fragment. In Figure 2 the spectrum of the complex liberated from the zeolite matrix is compared with that of a solution of $[Ru(bpy)_2bpz\text{-}Ru(NH_3)_5](PF_6)_4$ which had been independently prepared. The fact that the spectra are virtually superimposable indicates that, despite the large excess of the

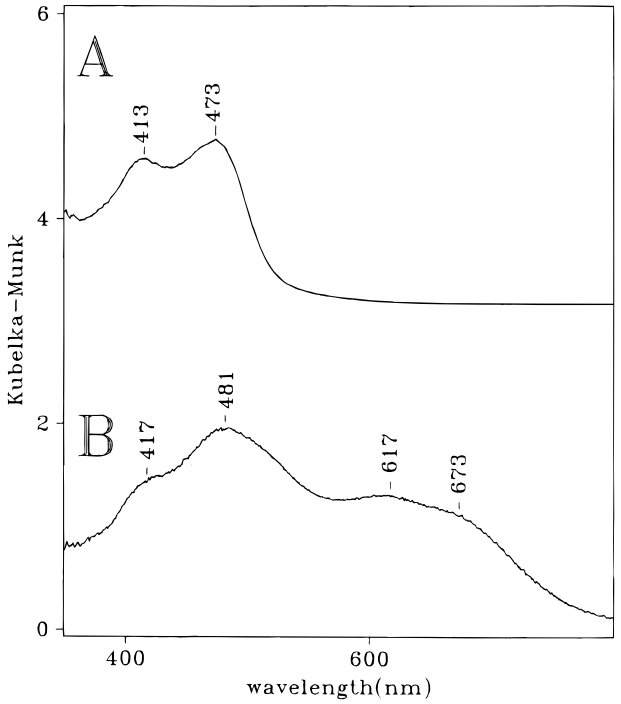

Figure 1. Diffuse reflectance spectra of Z-Ru(bpy)$_2$(bpz) (trace A) and of Z-Ru(bpy)$_2$bpz-Ru(NH$_3$)$_5$ (trace B).

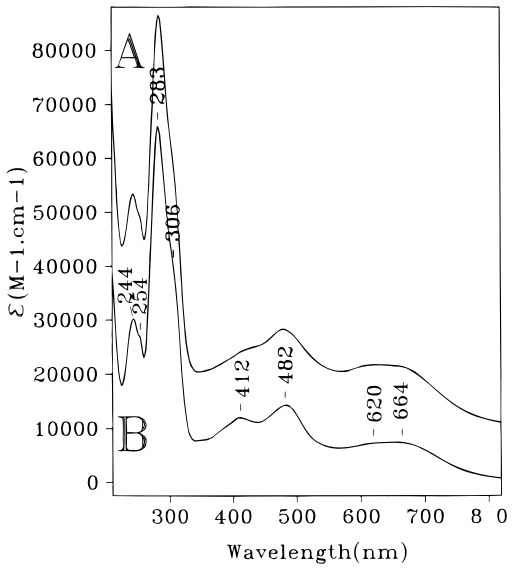

Figure 2. Electronic absorption spectra of [Ru(bpy)$_2$(bpz)-Ru(NH$_3$)$_5$]$^{4+}$ extracted from zeolite (trace A) and independently prepared [Ru(bpy)$_2$-(bpz)-Ru(NH$_3$)$_5$]$^{4+}$ (trace B). Intensity axis applies to trace B.

[Ru(NH$_3$)$_5$(H$_2$O)](PF$_6$)$_2$ used for the reaction with Z-Ru(bpy)$_2$-bpz, only one of the peripheral nitrogens of the bipyrazine reacts with the reagent to form Z-Ru(bpy)$_2$bpz-Ru(NH$_3$)$_5$. It seems most reasonable to attribute this lack of reactivity toward a second equivalent of the (positively charged) reagent to electrostatic factors, given that the mono-derivatized complex carries a 4+ charge and neighboring supercages have a negatively charged framework. Also, there may be steric constraints imposed on the entrapped Ru(bpy)$_2$bpz^{2+} molecule by the Y-zeolite supercage; i.e., it may be that only a single peripheral nitrogen of the bipyrazine is accessible to the Ru-(NH$_3$)$_5$(H$_2$O)$^{2+}$ ions (which occupy cages adjacent to the entrapped Ru(bpy)$_2$bpz^{2+} complex) during the reaction. Considering that the size of the mononuclear complex Ru-(bpy)$_2$bpz^{2+} is ∼12 Å[18] and the size of a single supercage is ∼13 Å, the binuclear complex Z-Ru(bpy)$_2$bpz-Ru(NH$_3$)$_5$ is not likely to fit into a single cage, but rather, the peripheral nitrogen and the externally coordinated fragment −Ru(NH$_3$)$_5$ most likely extend into the neighboring supercage through the ∼7 Å opening.

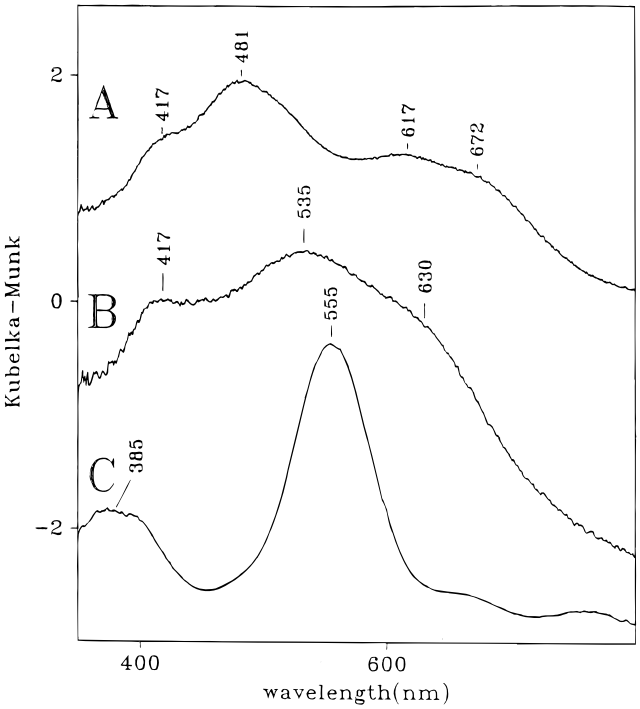

Figure 3. Diffuse reflectance spectra of Z-Ru(bpy)$_2$bpz-Ru(NH$_3$)$_5$ (trace A), Z-Ru(bpy)$_2$bpz-Ru(NH$_3$)$_5$ contaminated with oxidation byproducts (trace B), and independently prepared Z-Ru-red (trace C).

As mentioned briefly in the Experimental Section, during the preparation and the purification of the Z-Ru(bpy)$_2$bpz-Ru(NH$_3$)$_5$, great care must be taken so that the reaction mixture, containing a large excess of [Ru(NH$_3$)$_5$(H$_2$O)](PF$_6$)$_2$, is handled under strictly anaerobic conditions. In Figure 3 are compared the spectra of pure Z-Ru(bpy)$_2$bpz-Ru(NH$_3$)$_5$ (trace A) and a sample exposed to traces of air (trace B) during the purification step. Although other oxidation byproducts might be present, the dominant impurity in the contaminated sample is expected to be the trimeric complex Ruthenium-red ([(NH$_3$)$_5$Ru^{III}−O−Ru^{IV}-(NH$_3$)$_4$−O−Ru^{III}(NH$_3$)$_5$]$^{6+}$), which forms upon oxidation of the [Ru(NH$_3$)$_5$(H$_2$O)](PF$_6$)$_2$. This complex is easily detectable in the reflectance spectrum (trace C), exhibiting a characteristic absorption band near ∼550 nm ($\epsilon_{540} \simeq 20000$),[19] which is strong compared to that for Ru(bpy)$_2$bpz-Ru(NH$_3$)$_5$, i.e., $\epsilon_{660} \simeq 7500$ ($\epsilon_{650} \simeq 6000$ for [Ru(bpz)$_3$-Ru(NH$_5$)](PF$_6$)$_4$).[12] Since such a band, or even a shoulder, cannot be detected in the spectrum given in trace A, the data suggest that, when sufficient care is taken during the synthesis, the formation of this impurity can be prevented.

B. Formation of the Z-{Ru(bpy)$_2$bpz}·{Ru(mmb)$_3$} Assembly. Upon treatment of the Z-Ru(bpy)$_2$bpz-Ru(NH$_3$)$_5$ with an excess of another chelating polypyridine ligand (e.g., 5-mmb = 5-methyl-2,2′-bipyridine), at elevated temperatures, the (originally) blue complex turns yellow (a color characteristic of zeolite-entrapped tris-ligated complexes). This color change indicates a rupturing of the peripheral N$_{bpz}$−Ru(NH$_3$)$_5$ bond of

(18) Rillema, D. P.; Jones, D. S.; Levy, H. A. *J. Chem. Soc., Chem. Commun.* **1979**, 849.

(19) Seddon, E. A.; Seddon, K. R. *The Chemistry of Ruthenium*; Elsevier: New York, 1984; p 150.

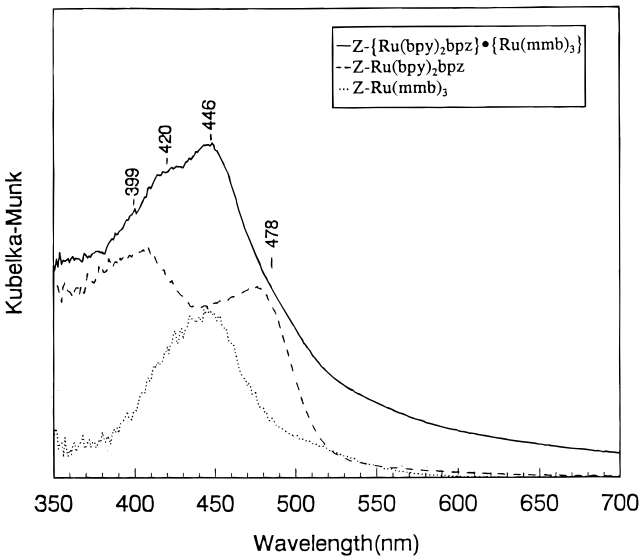

Figure 4. Diffuse reflectance spectra of Z-{Ru(bpy)$_2$bpz}·{Ru(mmb)} assembly (solid line), independently prepared Z-Ru(bpy)$_2$bpz (dashed line), and independently prepared Z-Ru(mmb)$_3$ (dotted line).

the Z-Ru(bpy)$_2$bpz-Ru(NH$_3$)$_5$ complex. The diffuse reflectance spectrum of the product of such a procedure is shown in Figure 4 (together with the diffuse reflectance spectra of independently prepared Z-Ru(bpy)$_2$bpz and Z-Ru(mmb)$_3$). From the spectrum it is evident that, the disappearance of the long wavelength absorption associated with the rupture of the peripheral bond in the Z-Ru(bpy)$_2$bpz-Ru(NH$_3$)$_5$ is accompanied by appearance of new bands associated with formation of Z-Ru(mmb)$_3$, which can be detected by its characteristic MLCT absorption at 446 nm.

While the diffuse reflectance spectrum of the AC assembly shown in Figure 4 discloses all the important features connected with the MLCT electronic excitation, the absorption characteristics in the region below 350 nm may be of interest as they may reveal the extent of sample contamination with the organic byproducts not removed during the extensive Soxhlet extraction. Since with the instrumentation available to us we are unable to measure the diffuse reflectance spectra in the UV region we employed the following approach to determine the extent of such contamination. The HF dissolved sample of the AC assembly was extracted into dichloromethane and the absorption spectra of the extracts in the 220−820 nm range were measured. If present, the organic impurities should be detected in the absorption spectrum of the organic extract. In Figure 5 are shown the absorption spectra of both the organic phase and the water phase after the extraction. As is apparent from the figure there is very weak absorption detected in the organic extract in the 220−350 region ($A_{288} \sim 0.05$). This absorbance is mainly due to the small amount of the complex dissolved in the organic phase (as indicated by weak absorption detected in the MLCT region). An identical observation has been made (spectra not shown) for the sample of the mechanical mixture following the same extraction procedure ($A_{288} \sim 0.09$). This result thus confirms that the extensive Soxhlet extraction can efficiently remove any organic byproducts from the Y-zeolite samples containing small concentrations of entrapped Ru(II)−polypyridine complex.

C. Resonance Raman Study of the Z-{Ru(bpy)$_2$bpz}·{Ru(mmb)$_3$} Assembly. To determine the relative abundance of the two complexes comprising the zeolite-entrapped assembly, we have acquired resonance Raman spectra of the assembly (AC), a sample of Z-Ru(mmb)$_3$, a sample of Z-Ru-

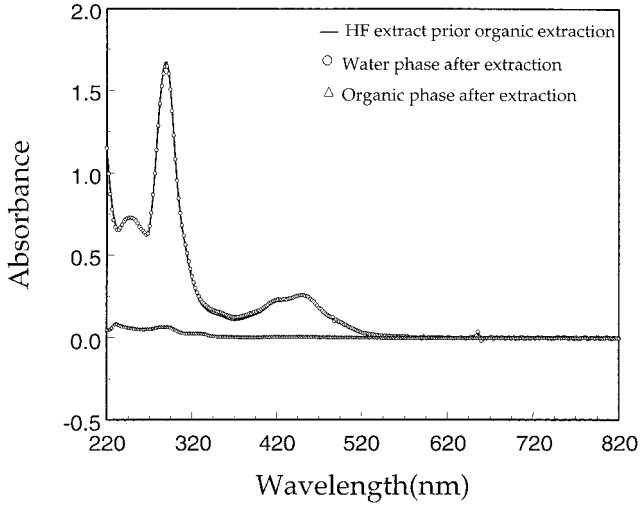

Figure 5. Electronic absorption spectra of the Z-{Ru(bpy)2bpz}·{Ru(mmb)$_3$} liberated from zeolite before and after extraction with CH_2Cl_2.

(bpy)$_2$bpz, and a sample (MM) prepared simply by mixing together the two single component zeolite samples; i.e., MM = 1 part Z-Ru(bpy)$_2$bpz + 1 part Z-Ru(mmb)$_3$. In all four cases the total "intrazeolitic concentration" of the complex was held constant at 16 μmol of complex per 1 g of zeolite, i.e., 1 complex per ∼30 supercages. For the samples used for preparation of MM (i.e., Z-Ru(bpy)$_2$bpz and Z-Ru(mmb)$_3$) the concentrations of entrapped complex were, prior the Raman study, determined independently by X-ray fluorescence[2e] and were found to be identical within experimental error. The results of the RR study are summarized in Figure 6. From a comparison of the traces corresponding to the Z-{Ru(bpy)$_2$bpz}·{Ru(mmb)$_3$} assembly and the mechanical mixture, it is evident that the relative intensities of the modes attributable to Ru(bpy)$_2$bpz^{2+} and the Ru(mmb)$_3^{2+}$, respectively, are virtually identical for these two samples. Given the fact that the ratio of the two complexes is 1:1 in the mechanical mixture of the Z-Ru(bpy)$_2$bpz and the Z-Ru(mmb)$_3$, we conclude that the Ru(bpy)$_2$bpz and the Ru(mmb)$_3$ are present in the same relative abundance in the Z-{Ru(bpy)$_2$bpz}·{Ru(mmb)$_3$} assembly. An essentially identical result was obtained for a synthetically randomized mixture (spectra not shown). Control studies, containing mixtures in a ratio of 1:1.2, gave distinctly different relative intensities; i.e., resonance Raman spectroscopy can detect differences in concentration of at least 20% in this particular case.

D. Electronic Emission Study of the Z-{Ru(bpy)$_2$bpz}·{Ru(mmb)$_3$} Assembly. The emission spectra of the series of zeolite-entrapped samples are shown in Figure 7. The emission spectra shown in Figure 7A were recorded from samples excited with the 472.7 nm excitation line, which is in closer resonance with the Ru(bpy)$_2$bpz^{2+} absorption maximum (at 473 nm) than with that of Ru(mmb)$_3^{2+}$ (absorption maximum at 446 nm). Consequently, the observed emission from the latter complex is much weaker. The emission spectra of the mechanical and randomized mixture are dominated by emission from Ru(bpy)$_2$bpz^{2+}, as expected. While there is only a moderate (∼10%) decrease in emission intensity when comparing the randomized and mechanical mixtures, there is a dramatic (∼4-fold) decrease in the observed emission intensity observed for adjacent cage assembly relative to the randomized mixture. In Figure 7B are shown the emission spectra for the same series of samples as in Figure 7A, except that the 457.9 nm excitation line was employed. In this case the excitation is closer to being

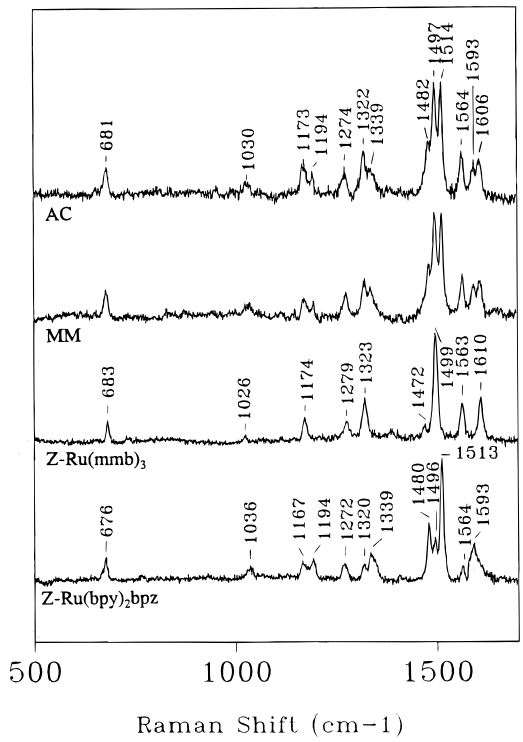

Figure 6. Resonance Raman spectra (with 457.9 nm excitation) of Z-Ru(bpy)$_2$bpz (16 μmol of complex/1 g of zeolite), Z-Ru(mmb)$_3$ (16 μmol/1 g), a 1:1 mechanical mixture of Z-Ru(bpy)$_2$bpz (16 μmol/1 g) and Z-Ru(mmb)$_3$ (16 μmol/1 g) (MM), and Z-{Ru(bpy)$_2$bpz}·{Ru(mmb)$_3$} assembly (8 μmol/1 g in Ru(bpy)$_2$bpz^{2+} and 8 μmol/1 g in Ru(mmb)$_3^{2+}$) (AC). A load of 16 μmol of complex/1 g of zeolite corresponds to 1 complex per ~30 cages.

in resonance with the MLCT absorption band of the Z-Ru(mmb)$_3$ than it is in the case of 472.7 excitation. Consequently, the observed emission intensity of Z-Ru(mmb)$_3$ is higher relative to Z-Ru(bpy)$_2$(bpz) when the 457.9 nm excitation is used. In this case also, there is a dramatic decrease of emission intensity observed for the adjacent cage assembly when compared to the randomized mixture (i.e., ~2.5-fold decrease).

The most important observation in this set of emission data is the significant decrease in emission intensity of the adjacent cage assembly (AC) compared to the mechanical mixture (MM) and the randomized mixture (RM). Following the procedure described in the Experimental Section, the relative total amounts of the entrapped complex for each of these three samples were determined by absorption spectroscopy and found to be quite similar (absorbancies at 446 nm were found to be 1.20, 1.29, and 1.12, respectively). Thus, in all three cases the same complexes, at the same overall concentration (within 10%), are entrapped within the zeolite matrix. The only difference lies in the unique spatial arrangement of the adjacent cage assembly, this arrangement apparently being solely responsible for the obvious emission intensity decrease. In other words, in the case of the mechanical mixture, each zeolite particle contains exclusively either Ru(bpy)$_2$bpz^{2+} or Ru(mmb)$_3^{2+}$, so that physical interaction between these complexes is not possible (it is noted here that the (Ru(bpy)$_2$bpz^{2+}−Ru(bpy)$_2$bpz^{2+}) and (Ru(mmb)$_3^{2+}$−Ru(mmb)$_3^{2+}$) pairs are still possible as two identical complexes can be coincidently entrapped in adjacent cages). In the case of the synthetically randomized mixture, a direct interaction between Ru(bpy)$_2$bpz^{2+} and Ru(mmb)$_3^{2+}$ can occur as there is a small (estimated ~5%),[20] but nonzero, probability that a fraction of these two complexes will be entrapped within adjacent zeolite supercages. It is suggested

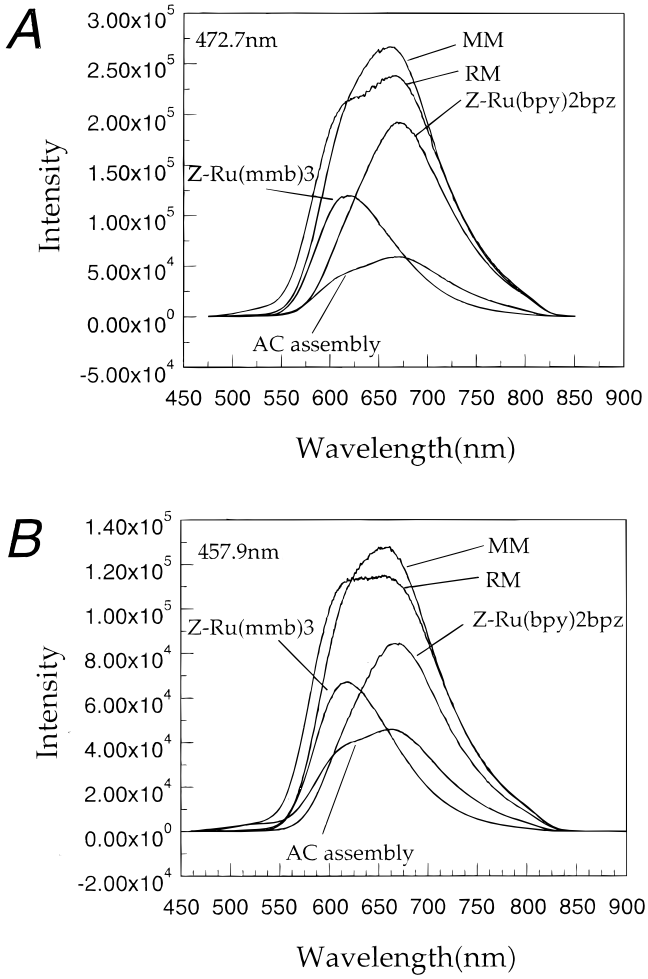

Figure 7. Electronic emission spectra for a series of zeolite-entrapped complexes. (A) Spectra recorded with 472.7 nm excitation. (B) Spectra recorded with 457.9 nm excitation. The loading of the complexes: Z-Ru(bpy)$_2$bpz (16 μmol of complex/1 g of zeolite), Z-Ru(mmb)$_3$, (16 μmol/1 g), a 1:1 mechanical mixture (MM) of Z-Ru(bpy)$_2$bpz (16 μmol/1 g) and Z-Ru(mmb)$_3$ (16 μmol/1 g), a synthetically randomized mixture (RM) of Z-Ru(bpy)$_2$bpz and Z-Ru(mmb)$_3$ (8 μmol/1 g in Ru(bpy)$_2$bpz^{2+} and 8 μmol/1 g in Ru(mmb)$_3^{2+}$), and a Z-{Ru(bpy)$_2$bpz}·{Ru(mmb)$_3$} assembly (AC) (8 μmol/1 g in Ru(bpy)$_2$bpz^{2+} and 8 μmol/1 g in Ru(mmb)$_3^{2+}$). A load of 16 μmol of complex/1 g of zeolite corresponds to 1 complex per ~30 cages. The emission intensities of samples containing a single complex (i.e., Z-Ru(bpy)$_2$bpz and Z-Ru(mmb)$_3$) are multiplied by a factor of 0.5 to account for the dilution effect. Spectra are not corrected for the spectrometer response.

here that the presence of these random adjacent pairs is responsible for the modest decrease in the emission intensity of the randomized compared to the mechanical mixture. In the adjacent cage assembly, however, both complexes are expected to occupy exclusively the adjacent supercages within the same zeolite particle. The observed ~2.5−4-fold emission intensity decrease of the adjacent cage assembly, compared to that of the random mixture, strongly suggests that a large fraction of the Ru(bpy)$_2$bpz^{2+} and Ru(mmb)$_3^{2+}$ complexes are entrapped within the interaction distance, i.e., within adjacent zeolite supercages. An accurate evaluation of the fraction of the adjacent Ru(bpy)$_2$bpz^{2+}−Ru(mmb)$_3^{2+}$ pairs in the AC sample from the observed emission intensities is not possible without further information about the nature and efficiency of the quenching mechanism.

(20) Sykora, M.; Castagnola, N. B.; Dutta, P. K.; Kincaid, J. R. *J. Phys. Chem.* Submitted for publication.

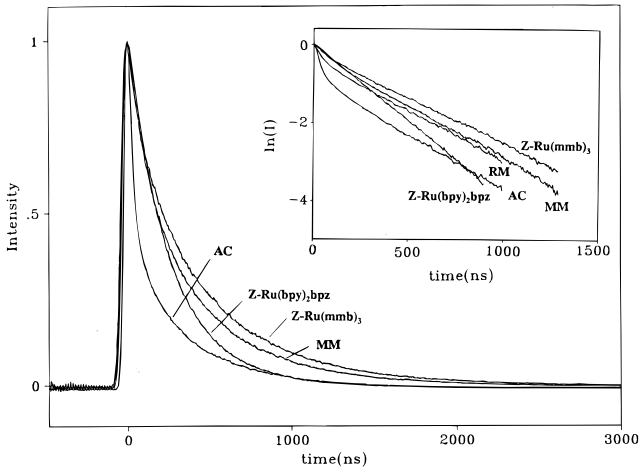

Figure 8. Electronic emission decay curves obtained at room temperature (with 354.7 nm excitation) for Z-Ru(bpy)$_2$bpz, Z-Ru(mmb)$_3$, a 1:1 mechanical mixture of Z-Ru(bpy)$_2$bpz and Z-Ru(mmb)$_3$ (MM), a synthetically randomized mixture of Z-Ru(bpy)$_2$bpz and Z-Ru(mmb)$_3$ (RM-inset only), and a Z-{Ru(bpy)$_2$bpz}·{Ru(mmb)$_3$} assembly (AC). Z-Ru(bpy)$_2$bpz, Z-Ru(mmb)$_3$, a 1:1 mechanical mixture of Z-Ru(bpy)$_2$bpz (16 μmol/1 g) and Z-Ru(mmb)$_3$ (MM), a synthetically randomized mixture of Z-Ru(bpy)$_2$bpz and Z-Ru(mmb)$_3$ (RM-insert only), and a Z-{Ru(bpy)$_2$bpz}·{Ru(mmb)$_3$} assembly (AC). The emission was monitored at 620 nm. The loading levels are the same as in Figure 6. The insert shows the same data plotted on a logarithmic scale.

Though an accurate estimate of this fraction is not possible, it is important to point out that the observed decrease in emission intensity, when considered in combination with the emission decay curves (vide infra), indicates that a substantial fraction of entrapped complexes in AC assembly occupy adjacent cages. Thus, as will be shown, the lifetime curves document the presence of a major component in the AC assembly only, which has a dramatically shorter lifetime (and correspondingly lower emission quantum yield) than those of the "isolated" complexes. The decreased emission intensity is therefore interpreted as a consequence of a decreased emission quantum yield for a significant fraction of entrapped complexes, which is ascribable to the introduction of an additional nonradiative decay pathway—quenching by the adjacent complex.

Additional evidence for high efficiency in the formation of adjacent pairs during the synthetic procedure is provided by comparison with results of a separate study[20] of the dependence of emission intensity on concentration for a series of zeolite-entrapped Ru(bpy)$_3^{2+}$ samples. In that study a comparable (~2.5-fold) decrease in emission intensity was observed between the sample with the lowest concentration (virtually all molecules isolated) and the highest concentration (no isolated molecules).

E. Excited-State Lifetime Study of the Z-{Ru(bpy)$_2$bpz}·{Ru(mmb)$_3$} Assembly. In an attempt to gain a better understanding of the processes responsible for the quenching of the emission intensity in the adjacent cage assembly, the emission decay curves for the five samples (Z-Ru(bpy)$_2$bpz and Z-Ru(mmb)$_3$, the mechanical mixture (MM), the random mixture (RM), and the adjacent cage assembly (AC)) have been analyzed. The observed emission decay curves for the samples studied are shown in Figure 8 (only the log plot being shown for RM). Comparison of the traces clearly indicates that the emission decays much more rapidly in the case of the adjacent cage assembly than in the case of the mechanical mixture. Moreover, the emission observed from the assembly decays even more rapidly than the emission observed from the relatively short-lived Z-*Ru(bpy)$_2$(bpz). This observation is clearly consistent with the observed dramatic decrease in the total emission intensity for the assembly discussed in the previous section. In the insert of Figure 8 are shown the same data plotted on the logarithmic scale. In this plot the slopes of the curves indicate the rate of the emission decay for a particular species. From the data, it can be shown that, in the case of the mechanical mixture, the emission decay curve at early times after the excitation (approximately the first 200−300 ns) is dominated by the emission from the *Ru(bpy)$_2$(bpz)$^{2+}$ component. At later times, the emission from *Ru(mmb)$_3^{2+}$ becomes the dominant contribution. Thus, the curve observed for the mechanical mixture can be well reproduced by simple numerical addition of the curves obtained independently for the single-component samples, i.e., Z-*Ru(bpy)$_2$bpz and Z-*Ru(mmb)$_3$. This kind of result is obviously expected when there is no interaction between the emitting species. The curve representing the decay of the emission from the adjacent cage assembly, however, differs quite distinctly from the one observed for the mechanical mixture. Although beyond ~500 ns after excitation the slopes of the two curves are virtually identical, at shorter times the curve for AC is more complex, suggesting the presence of a very short-lived component that dominates the decay curve at times below ~100 ns. Although the trace corresponding to emission decay from the synthetically randomized mixture shows behavior very similar to that observed for MM, the trace corresponding to RM could not be reproduced by simple numerical addition of traces for the single component samples, the deviation being most apparent at times below ~200 ns. It is suggested here that this deviation (which is also apparent upon close examination of the traces in the insert of Figure 8) is due to a small contribution of a short-lived component to the observed emission decay which is, however, much smaller than it is in the case of AC. As was pointed out earlier, such a contribution is naturally expected for the RM sample inasmuch as a small fraction of the complexes are expected (from statistical considerations)[20] to be involved in adjacent cage (Ru(bpy)$_2$bpz^{2+}−Ru(mmb)$_3^{2+}$) type interactions.

Table 1. Excited State Components and Lifetimes[a]

species	$\tau_1(I_{01})$	$\tau_2(I_{02})$	$\tau_3(I_{03})$	$\tau_4(I_{04})$
1. Z-Ru(bpy)$_2$bpz		225(100)		
2. Z-Ru(mmb)$_3$	515(70)		110(30)	
3. MM[b]	530(43)	220(38)	90(19)	
4. RM[c]	570(52)	205(26)	77(22)	
5. AC[d]	530(20)	210(24)		30(56)

[a] I_{0i} represents the relative contribution of the ith component to the total emission intensity. [b] Mechanical mixture (1:1) of Z-Ru(bpy)$_2$bpz and Z-Ru(mmb)$_3$. [c] Synthetically randomized mixture Z-Ru(bpy)$_2$bpz/Z-Ru(mmb)$_3$. [d] Adjacent cage assembly Z-{Ru(bpy)$_2$bpz}·{Ru(mmb)$_3$}.

$$I = \sum_{i=1}^{n} I_{0i} \exp(-t/\tau_i) \qquad (n = 1, 3)$$

To resolve the observed differences quantitatively, the experimental curves were analyzed by numerical fitting to an appropriate kinetic model. As a first approximation we have chosen the multiexponential expression, which, when compared to other kinetic models, had been shown[3b,7b,c,8,20] to give best fits for data recorded from Y-zeolite entrapped species. In this model τ_i is the lifetime of the component "i" and I_{0i} is the initial intensity of the component "i" at time $t = 0$. The results of this analysis are summarized in Table 1. In the case of Z-Ru(bpy)$_2$bpz, the emission curve was fit satisfactorily with a monoexponential expression with the extracted value for $\tau_1 =$

Table 2. Estimated Energetics of Possible Quenching Processes

1. electron transfer	
a. ES-GS	
$*Ru(bpy)_2bpz^{2+} + Ru(mmb)_3^{2+} \rightarrow Ru(bpy)_2bpz^{3+} + Ru(mmb)_3^{+}$	$\Delta G° = 0.89$ eV
$*Ru(bpy)_2bpz^{2+} + Ru(mmb)_3^{2+} \rightarrow Ru(bpy)_2bpz^{+} + Ru(mmb)_3^{3+}$	$\Delta G° = 0.13$ eV
$*Ru(mmb)_3^{2+} + Ru(bpy)_2bpz^{2+} \rightarrow Ru(mmb)_3^{3+} + Ru(bpy)_2bpz^{+}$	$\Delta G° = 0.03$ eV
$*Ru(mmb)_3^{2+} + Ru(bpy)_2bpz^{2+} \rightarrow Ru(mmb)_3^{+} + Ru(bpy)_2bpz^{3+}$	$\Delta G° = 0.78$ eV
b. ES-ES	
$*Ru(bpy)_2bpz^{2+} + *Ru(mmb)_3^{2+} \rightarrow Ru(bpy)_2bpz^{3+} + Ru(mmb)_3^{+}$	$\Delta G° = -1.16$ eV
$*Ru(bpy)_2bpz^{2+} + *Ru(mmb)_3^{2+} \rightarrow Ru(bpy)_2bpz^{+} + Ru(mmb)_3^{3+}$	$\Delta G° = -1.92$ eV
2. energy transfer	
$*Ru(bpy)_2bpz^{2+} + Ru(mmb)_3^{2+} \rightarrow Ru(bpy)_2bpz^{2+} + *Ru(mmb)_3^{2+}$	$\Delta G° = 0.12$ eV
$*Ru(mmb)_3^{2+} + Ru(bpy)_2bpz^{2+} \rightarrow Ru(mmb)_3^{2+} + *Ru(bpy)_2bpz^{2+}$	$\Delta G° = -0.12$ eV

[a] The listed $\Delta G°$ values are calculated by using the reported values of the ground and excited-state redox potentials, for each complex, as listed in ref 6c. Since the values for $Ru(mmb)_3^{2+}$ are not reported the values used in this table were obtained by interpolation between the values reported for $Ru(bpy)_3^{2+}$ and $Ru(dmb)_3^{2+}$ (dmb = 4,4′-dimethyl-2,2′-bipyridine).

225 ns. In the case of Z-$Ru(mmb)_3$, the use of a biexponential ($n = 2$) expression was necessary in order to obtain a satisfactory fit. The best fit yielded lifetimes of $\tau_1 = 515$ ns for a dominant component and $\tau_2 = 110$ ns for a minor component. While the former is assigned to the excited-state lifetime of the isolated Z-*$Ru(mmb)_3$, the latter is possibly connected with the emission from the $*Ru(mmb)_3^{2+}$ molecules which are coincidently entrapped within the interaction distance of another $Ru(mmb)_3^{2+}$ or $*Ru(mmb)_3^{2+}$ molecule, i.e., are affected by a self-quenching process. While a similar process might be expected to occur for the Z-$Ru(bpy)_2(bpz)$ samples, the relative probability for self-quenching may be lower than that for Z-$Ru(mmb)_3$. In fact, results of studies of the emission decay for a relatively large number of zeolite-entrapped complexes indicated that the relative contribution of the short component varies for different complexes.[3b,7b,c,8] In this regard, it should be pointed out that, in the case of Z-$Ru(bpy)_2(bpz)$, the ^{3}MLCT state is expected to be more asymmetrical than that of Z-$Ru(mmb)_3$ (or other tris-homoleptic complexes) over time periods which are long compared to the electron hopping rate. Thus, the ^{3}MLCT of Z-$Ru(bpy)_2(bpz)$ is localized on the bpz ligand and there exists a barrier to population of the (higher energy) bpy-localized state.[21] For tris-homoleptic complexes, such as $Ru(mmb)_3^{2+}$, electron hopping is expected to be efficient and the resulting rapid charge relocation may facilitate interactions with nearby complexes and thereby lead to a greater contribution of the short component.

In the case of the adjacent cage assembly, the emission curve is dramatically changed, relative to that of MM, because of the presence of a dominant short-time component ($\tau_4 = 30$ ns). Inasmuch as no evidence for such a short-lived component was found for the MM sample, it is obviously attributable to interactions within the adjacent cage dyads. In the case of the synthetically randomized mixture the short component $\tau_4 \sim 30$ ns was not extracted from the numerical analysis as satisfactory fits were obtained with a three- rather than a four-exponential model. It is suggested here, however, that the $\tau_3 = 77$ ns component is a "mixture" of the short −30 ns component and intermediate ∼100 ns component detected in samples of Z-Ru-$(mmb)_3$ and MM; i.e., the short and intermediate components are not resolved due to their comparable lifetimes and small contribution (only ∼5% of $Ru(bpy)_2bpz^{2+}$ and $Ru(mmb)_3^{2+}$ are expected to form adjacent pairs and thus contribute to the $\tau_4 \sim$ 30 ns component).[20] Although the short component most likely contributes to the emission decay observed for the randomized mixture, its contribution (and thus the fraction of $Ru(bpy)_2bpz^{2+}$ and $Ru(mmb)_3^{2+}$ adjacent pairs) is apparently insignificant compared to that of the AC assembly.

The present, rather simplified, analysis would indicate that, in the case of adjacent cage assembly, at least 60% of the excited state population decays by this more rapid process. We wish to emphasize that this estimate of 60% is the minimum fraction of adjacent pairs. To the extent that members of adjacent pairs may decay by the normal, slower route, this fraction may be very much underestimated. A better estimate will require an in-depth analysis of a more complete set of experimental data, including time-resolved diffuse reflectance and emission measurements conducted over a range of excitation and emission wavelengths. While such experiments are needed to determine the nature of the rapid quenching process, it is interesting to consider various possible decay mechanisms and their (estimated) thermodynamic parameters. Table 2 summarizes the energetics involved for several processes by which the two components of an adjacent cage dyad might interact and depopulate excited state(s). From the table it is clear that the most energetically favorable process is electron-transfer quenching of two adjacent ^{3}MLCT states. However, as efforts have been made here to employ low incident intensities for both the emission spectra and the lifetime measurements, it seems unlikely that a significant population of "doubly excited" dyads would be encountered. Energy transfer from $*Ru(mmb)_3^{2+}$ to $Ru(bpy)_2(bpz)^{2+}$ is also slightly favorable energetically. Though electron transfer quenching of an excited state by an adjacent ground state species is apparently energetically prohibited, in two cases the energetics are not strongly unfavorable ($\Delta G° =$ 0.03 and 0.13 eV, i.e., oxidative quenching of $*Ru(mmb)_3^{2+}$ and reductive quenching of $*Ru(bpy)_2(bpz)^{2+}$, respectively). In fact, these types of estimates are necessarily rather crude approximations for $\Delta G°$, since ground- and excited-state redox potentials for complexes *inside* the zeolite framework are not readily available. Given this situation, it is entirely possible that both of the electron-transfer processes between a ^{3}MLCT state and the adjacent ground state partner might actually be energetically favorable. Similarly, the energy transfer between the $Ru(mmb)_3^{2+}$ and $Ru(bpy)_2(bpz)^{2+}$ is quite feasible, especially considering the fact that two complexes entrapped in adjacent zeolite cages are in near physical contact, favoring the short-range (Dexter type) interactions.

Conclusions

The present report summarizes synthetic procedures to construct dyads of ruthenium polypyridine complexes within the supercage framework of Y-zeolite. Spectroscopic evidence

(21) (a) Danzer, G. D.; Kincaid, J. R. *J. Phys. Chem.* **1990**, *94*, 3976. (b) Gex, J. N.; DeArmond, M. K.; Hanck, K. W. *J. Phys. Chem.* **1987**, *91*, 251. (c) Myrick, M. L.; Blakley, R. L.; DeArmond, M. K.; Arthur, M. L. *J. Am. Chem. Soc.* **1988**, *110*, 1325. (d) Bargawi, K. R.; Akasheh, T. S.; Beaumont, P. C.; Parsons, B. J.; Phillips, G. O. *J. Phys. Chem.* **1988**, *92*, 291.

confirms the identity of anticipated intermediate or precursor complexes and documents the expected relative concentrations of the two terminal complexes (i.e., $Ru(bpy)_2(bpz)^{2+}$ and $Ru(mmb)_3^{2+}$). Comparison of photophysical data for the assembly with those for a simple mechanical mixture and a synthetic randomized mixture of the two zeolite-entrapped complexes provides convincing evidence for the existence of a significant interaction between the adjacent cage dyad components which leads to dramatic effects on the total emission intensity and the shapes of the emission decay curves.

While further experiments will be needed to establish the precise nature of this additional relaxation process, thermodynamic considerations using approximate estimates of ground- and excited-state redox potentials would seem to suggest that a number of electron-transfer quenching processes might participate. In fact, such a conclusion is consistent with results of initial studies of photoinduced electron-transfer quenching by acceptors loaded into the remaining supercages, wherein it was shown that net charge separation increased by a factor of about 4 for these zeolite assemblies, relative to the net charge separation observed for the mechanical mixture.[22]

Acknowledgment. This work was supported by a grant from the Division of Chemical Sciences, U.S. Department of Energy (Grant No. DE-FG-02-86ER13619).

JA9635847

(22) Sykora, M.; Kincaid, J. R. *Nature* **1997**, *387*, 162.